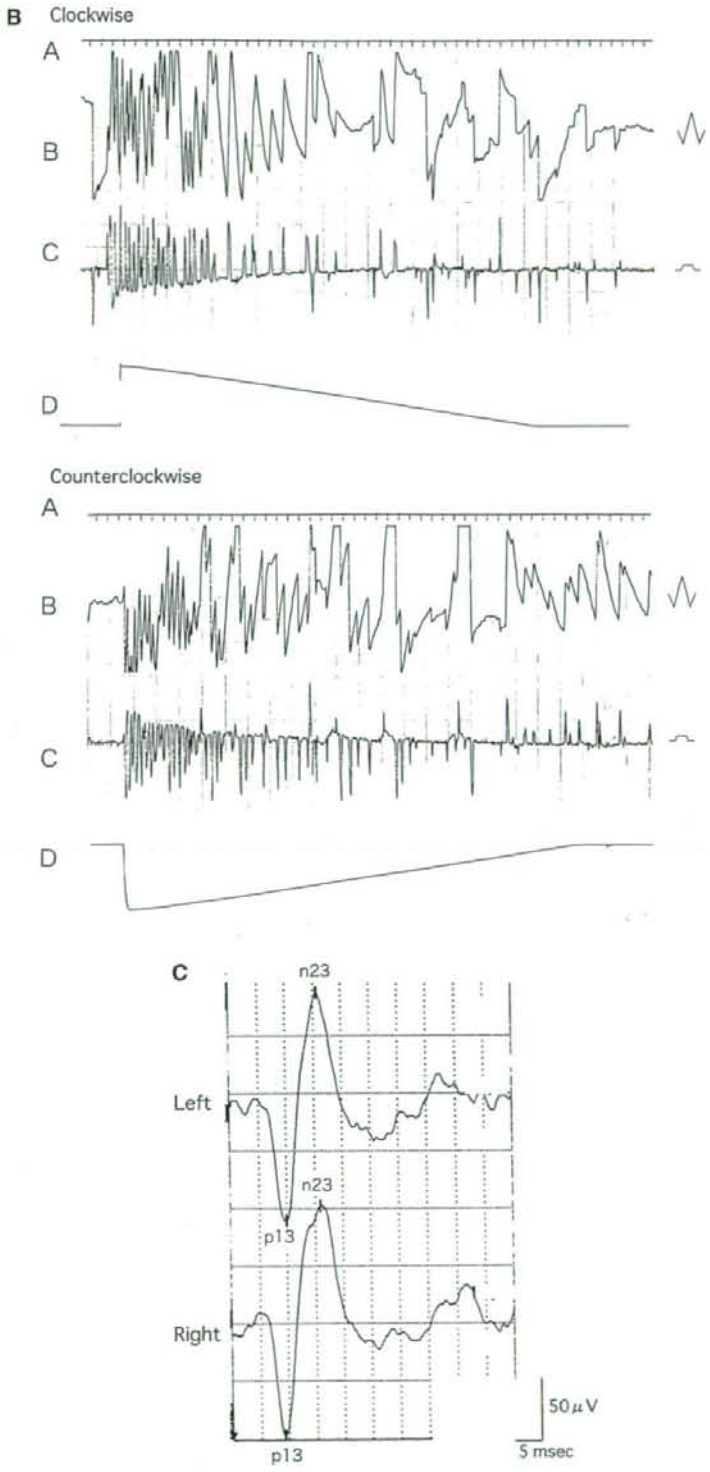

Figure 2 (*Continued*)

Rotational chair test

Fourteen patients (70%) showed normal responses during rotation in both directions. One patient showed normal responses during rotation in one direction, but poor responses in the opposite direction. Two patients showed poor responses in both directions, and three showed no responses in any direction.

VEMP test

Ten patients (50%) showed normal responses bilaterally. Six patients (30%) showed asymmetrical responses. Four patients (20%) showed no responses bilaterally.

Classification of patients

We classified the patients into four groups.

Group A. Normal vestibular function group. Three patients (15%; nos 1–3) showed normal responses bilaterally in the caloric test, rotational chair test and VEMP recording. Figure 1 shows the representative results of vestibular tests for patient no. 1.

Group B. Asymmetrical caloric response group. Seven patients (35%; nos 4–10) showed asymmetrical responses in the caloric test despite normal responses in the rotational chair test and VEMP recording bilaterally. Figure 2 shows the representative results for patient no. 4.

Group C. Poor or non-caloric response group. Five patients (25%; nos 11–15) showed poor or no responses in the caloric test bilaterally, but showed normal responses in the rotational chair test and showed normal or decreased reproducible VEMPs. Figure 3 shows the representative results for patient no. 15.

Group D. Absent-function group. Five patients (25%; nos 16–20) showed no responses in the caloric test, rotational chair test and VEMP recording. Figure 4 shows the representative results for patient no. 20.

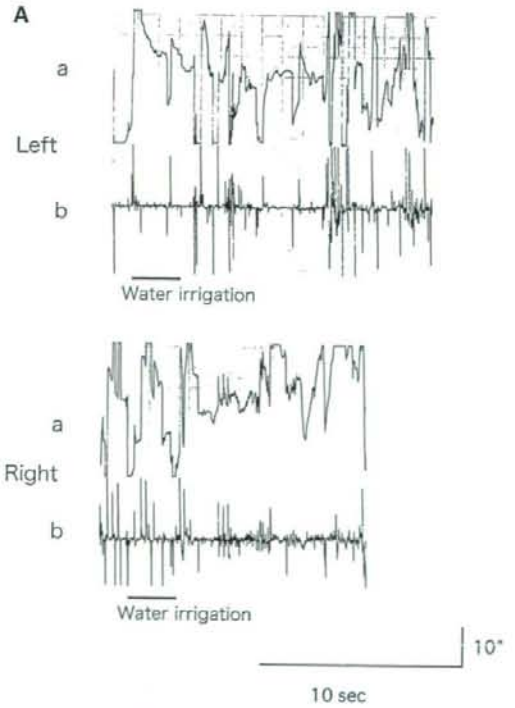

Figure 3. (A) Ice-water caloric test of patient no. 15. No significant response is found. Time constants: a, 3.0 s; b, 0.03 s. (B) Rotational chair test of patient no. 15. Both sides show normal responses. A, Time scale (one division per second); B, Angular displacement of eyes (time constant, 3.0 s; calibration signal, 10°); C, Rotational velocity of eyes (time constant, 0.003 s; calibration signal, 20° /s); D, Angular velocity of chair rotating. (C) VEMP of patient no. 15. On the right side, normal response is shown, but the left side shows decreased response.

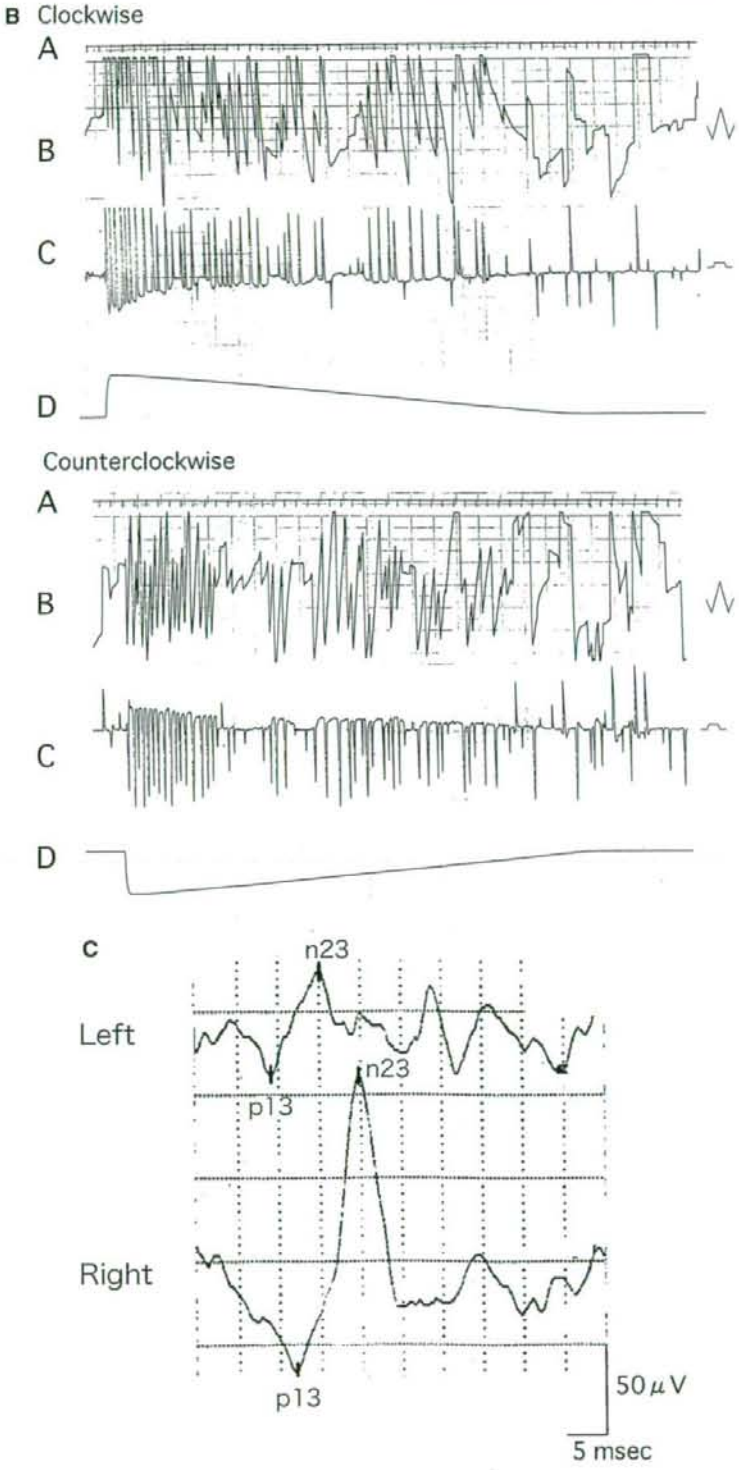

Figure 3 (*Continued*)

The proportions of the groups in three vestibular function tests are shown in Figure 5.

Discussion

In adults, bilateral vestibular dysfunction may be manifested as postural unsteadiness, but the loss of postural control is rare so long as visual cues are available. In infants and young children with hypoactive labyrinths, however, the loss of postural control is much more common and the development of gross motor function is delayed [11,12]. Kaga et al. revealed the hypo-reaction or non-reaction in the rotational chair test in infants, in whom the achievements of head control and independent walking were delayed, and pointed out vestibular involvement in gross motor function and the significance of vestibular assessments of hearing impaired infants [13].

In this study, we carried out the vestibular assessment of infants and children with congenital and acquired deafness by the caloric test, rotational chair test and VEMP recording. Among the patients, 85% showed abnormal responses in at least one test. Regarding the ice-water caloric test, 10 patients (50%) showed caloric hypofunction or areflexia. The proportion of caloric hypo- or areflexia was slightly higher than those in several previous studies [1–3,9], which ranged from 20% to 40%. This may be explained by the fact that all of our patients had a severe hearing loss and were scheduled to undergo CI. According to recent research [14,15], nearly 70% of cochlear implant patients showed no or low intensity responses in caloric irrigation before operation.

As regards the rotational chair test, our study demonstrated that 70% of the patients showed normal responses. That is, some patients (group C, 25%) showed normal responses in the rotational chair test despite their hypo- or areflexia in the caloric test. This result is inconsistent with that of the study of Tribukait et al. [9], in which their subjects showing no caloric responses did not show any nystagmus on rotation. The rotational chair test at higher frequencies may stimulate the semicircular canals and otolith organs in both ears simultaneously, whereas the caloric test stimulates only one horizontal semicircular canal at a time. The rotational chair test may possibly stimulate labyrinths including

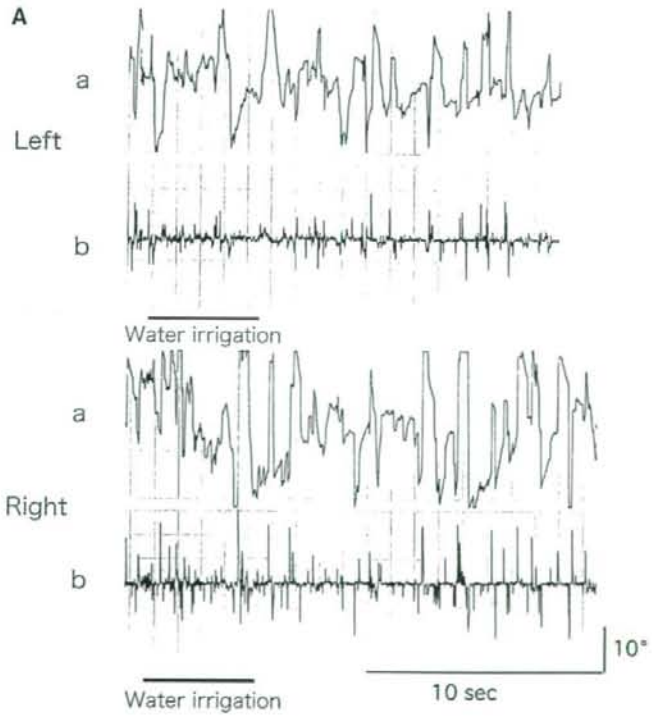

Figure 4. (A) Ice-water caloric test of patient no. 20. No response is found. Time constants: a, 3.0 s; b, 0.03 s. (B) Rotational chair test of patient no. 20. No response is found. A, Time scale (one division per second); B, Angular displacement of eyes (time constant, 3.0 s; calibration signal, 10°); C, Rotational velocity of eyes (time constant, 0.03 s; calibration signal, 20° /s); D, Angular velocity of chair rotating. (C) VEMP of patient no. 20. No reproducible responses are found.

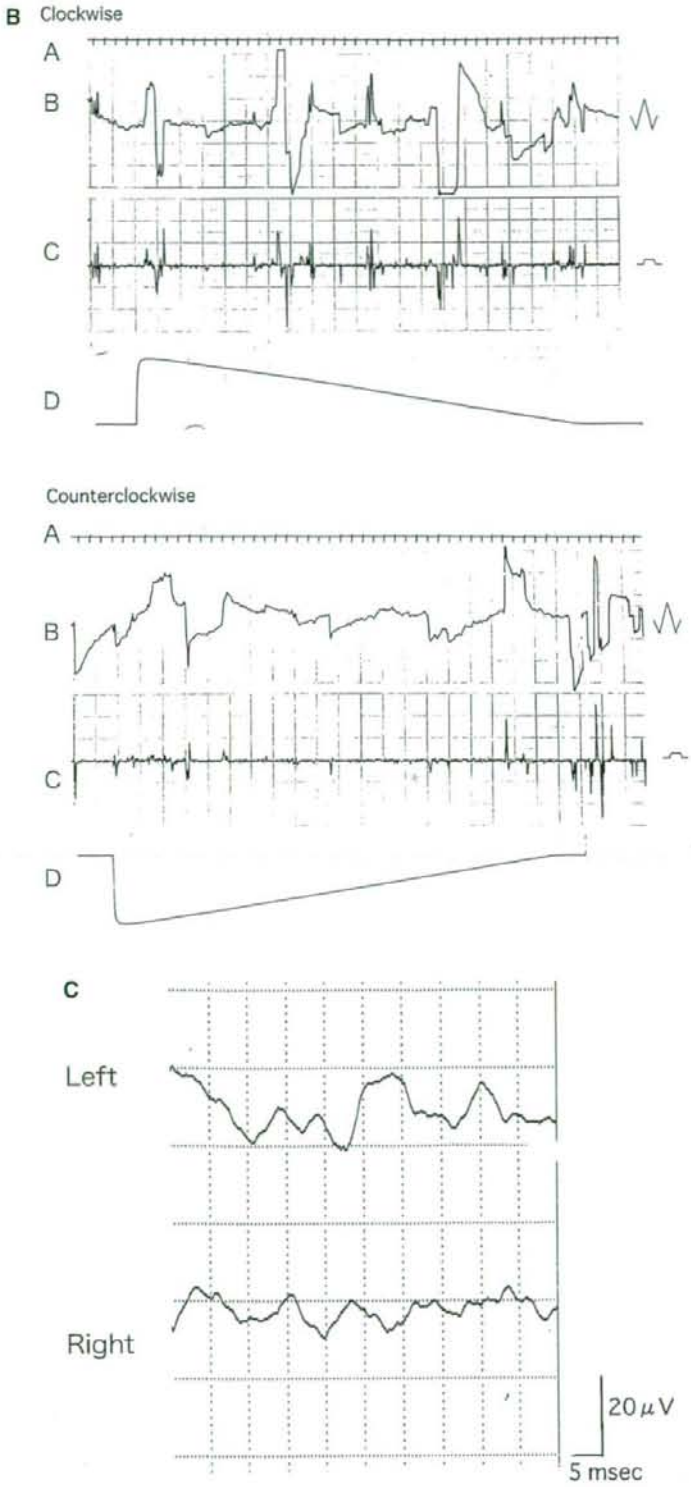

Figure 4 (*Continued*)

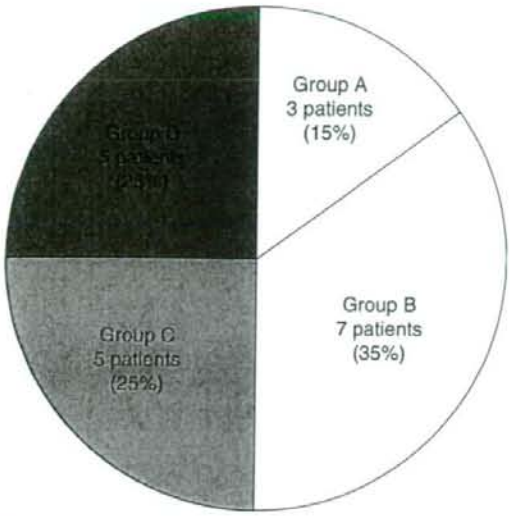

Figure 5. Proportions of four groups for three vestibular function tests. Group A: normal vestibular function group. Group B: asymmetrical caloric response group. Group C: poor or non-caloric response group. Group D: absent-function group.

three semicircular canals and otolith organs on both sides more strongly than the caloric test; thus, it will be able to detect the remaining weak vestibular function.

In VEMP recording, as one of the succulus tests, 50% of children showed normal responses bilaterally, 30% asymmetrical responses and 20% no responses. There are very few comparable data in the literature; however, these results are very similar to those of the VEMP study of Tribukait et al. [9]. Despite the difference in the children's age, the proportions of their patients showing normal responses bilaterally, asymmetrical responses and no responses were 58%, 17% and 25%, respectively. According to these results, the succular function is supposed to be mature even at this early age of childhood.

Among the three tests for vestibular assessment in our study, all the children in the group who showed normal responses bilaterally or asymmetrically in the caloric test showed normal responses in the rotational chair test and VEMP recording (groups A and B), and all of the children in the group who showed poor or no responses in the rotational chair test failed to show any response in caloric test and VEMP recording (group D). There were some patients who showed normal responses in the rotational chair test and VEMP recording but showed caloric hypo- or areflexia (group C). These results suggest that the semicircular function is more vulnerable than the otolith function.

In our study, four of five patients in group D and one of five patients in group C showed off-the-scale hearing. In contrast, in groups A and B, no patients showed off-the-scale hearing. Sandberg and Terkildsen [16] associated caloric responses with the pure tone audiogram of each individual ear in 57 children with some residual hearing, and in the group with very poor hearing (>98 dB) only 20% showed normal caloric responses, whereas among the ears with less severe hearing loss (<90 dB) the caloric responses were normal in 80%. Almost all of our patients showed a very severe hearing loss of >95 dB, and those in group D seemed to show the worst hearing level. The otolith function is likely preserved despite the severe hearing loss, yet the patients with off-the-scale hearing tend to have a poor vestibular function not only in the semicircular canals but also in the saccules.

The problems and difficulties encountered in measuring vestibular function in this study were as follows. It was difficult to obtain younger children's cooperation during these tests and to observe their responses, because the procedures often elicited startle responses or crying [13]. Concerning the VEMP recording procedure in infants, it was difficult to maintain the same level of muscle contraction and the desired EMG activity, and help was necessary for positioning and maintaining the muscle contraction level, as reported previously [17].

Hearing impairment is frequently accompanied by a disruption in balance and orientation functions, but this latter function is rarely assessed in infants and young children. In recent years we have noted an increased recognition of the need for early and aggressive habilitation of hearing impaired children. Comprehensive evaluations – including but not limited to auditory, neurological, and intellectual states – are essential for implementing an individualized habilitation plan. In view of the prevalence of vestibular hypofunction among these children and its impact on their early development, we concur that vestibular assessment is essential and important for patients.

In recent years, many deaf children worldwide have undergone CI in their early childhood. After CI, owing to the electrode wire inserted into the cochlea, cochlear and vestibular sensory cells are likely damaged [10,18]. The vestibular assessment of infants and young children is difficult to perform, but it must offer highly important information before and after CI.

Finally, we conclude that 85% of infants and young children who had a severe hearing loss showed abnormal results in the vestibular assessment using the caloric test, rotational chair test and VEMP

recording. We emphasize that the peripheral vestibular system including semicircular canals and saccules of deaf infants and children should be examined. The results of these tests are highly beneficial for the management of hearing impaired children.

References

[1] Arnvig J. Vestibular function in deafness and severe hardness of hearing. Acta Otolaryngol (Stockh) 1955;45:283–8.

[2] Everberg G. Unilateral total deafness in children: clinical problems with special view to vestibular function. Acta Otolaryngol (Stockh) 1960;52:253–69.

[3] Goldstein R, Landau WM, Kleffner FR. Neurologic assessment of some deaf and aphasic children. Ann Otol Rhinol Laryngol 1958;67:468–79.

[4] Yakushin SB, Raphan T, Suzuki J, Arai Y, Cohen B. Dynamics and kinematics of the angular vestibulo-ocular reflex in monkey: effects of canal plugging. J Neurophysiol 1998;80:3077–99.

[5] Angelaki DE, Newlands SK, Dickman JD. Inactivation of semicircular canals causes adaptive increases in otolith-driven tilt responses. J Neurophysiol 2002;87:1635–40.

[6] Colebatch JG, Halmagyi GM, Skuse NF. Myogenic potentials generated by a click-evoked vestibulocollic reflex. J Neurol Neurosurg Psychiatry 1994;57:190–7.

[7] Murofushi T, Halmagyi GM, Yavor RA, Colebatch JG. Absent vestibular evoked myogenic potentials in vestibular neurolabyrinthitis: an indicator of inferior vestibular nerve involvement? Arch Otolaryngol Head Neck Surg 1996;122: 845–8.

[8] Murofushi T, Curthoys IS. Physiological and anatomical studies of click-sensitive primary vestibular afferents in the guinea pig. Acta Otolaryngol (Stockh) 1997;117:66–72.

[9] Tribukait A, Brantberg K, Bergenius J. Function of semicircular canals, utricle and saccules in deaf children. Acta Otolarygol (Stockh) 2004;124:41–8.

[10] Jin Y, Nakamura M, Shinjo Y, Kaga K. Vestibular-evoked myogenic potentials in cochlear implant children. Acta Otolaryngol (Stockh) 2006;126:164–9.

[11] Rapin I. Hypoactive labyrinths and motor development. Clin Pediatr 1974;13:922–37.

[12] Eviatar L, Eviatar A. Neurovestibular examination of infants and children. Adv Otorhinolaryngol 1978;23:169–91.

[13] Kaga K, Suzuki J, Marsh RR, Tanaka Y. Influence of labyrinthine hypoactivity on gross motor development of infants. Ann N Y Acad Sci 1981;374:412–20.

[14] Ito J. Influence of the multichannel cochlear implants on vestibular function. Otolaryngol Head Neck Surg 1998;118: 900–2.

[15] Buchman GA, Joy J, Hodges A, Telischi FF, Balkany TJ. Vestibular effects of cochlear implantation. Laryngoscope 2004;114:1–22.

[16] Sandberg LE, Terkildsen K. Caloric tests in deaf children. Arch Otolaryngol 1965;81:350–4.

[17] Sheykholesami K, Kaga K, Megerian CA, Arnold JE. Vestibular-evoked myogenic potentials in infancy and early childhood. Laryngoscope 2005;115:1440–4.

[18] Tien HC, Linthicum FH Jr. Histopathologic changes in the vestibule after cochlear implantation. Otolaryngol Head Neck Surg 2002;127:260–4.

A magnetoencephalographic study of Japanese vowel processing

Erika Ogata[a], Masato Yumoto[b], Kenji Itoh[c], Sotaro Sekimoto[c], Shotaro Karino[d] and Kimitaka Kaga[a,d]

Departments of [a]Sensory and Motor Neuroscience, [b]Clinical Laboratory, [c]Speech and Cognitive Science and [d]Otolaryngology, Graduate School of Medicine, University of Tokyo, Tokyo, Japan

Correspondence and requests for reprints to Erika Ogata, MS, Sensory and Motor Neuroscience, Graduate School of Medicine, University of Tokyo, 7-3-1 Hongo, Bunkyo-ku, Tokyo 113-8655, Japan
Tel: +81 3 5800 8665; fax: +81 3 3814 9486; e-mail: ogatae-tky@umin.ac.jp

Received 26 April 2006; accepted 17 May 2006

Magnetic brain responses were recorded to clarify the cortical representation of vowel processing in Japanese. We investigated the peak latencies and equivalent current dipoles of the auditory N1m responses to the Japanese vowels [a], [i], [o], and [u]. In intraindividual analyses for a single participant, well-replicated results for the dipole parameters supported the existence of phoneme-specific cortical maps for vowels. In the interindividual analyses for the eight participants, [a] and [i] elicited significantly earlier N1m responses than [u], and the dipole for [i] was more posteriorly oriented than [a] in the left hemisphere. The results of the current study suggest left hemispheric predominance in vowel processing and that factors associated with a different language system may modify the cortical map. *NeuroReport* 17:1127–1131 © 2006 Lippincott Williams & Wilkins.

Keywords: magnetoencephalography, N1m, phoneme processing, vowels

Introduction

Recently, several studies have examined cortical activity during the processing of vowel sounds by means of magnetoencephalography (MEG) [1–9]. In these studies, N1m (the magnetic counterpart of the auditory-evoked N1 potential) was used as an index of vowel sound processing. Previous studies reported a difference in equivalent current dipoles (ECDs) for N1m responses to vowels and pure tones [2,4], and a latency difference for vowel types [8]. These results were considered to be evidence suggesting the distinct processing patterns of vowels in humans. Some experiments support the notion that the ECD locations for N1m may reflect a distinct cortical representation of vowel sounds [1,3,5,6,9]. The changes in ECD localization for each vowel, which had not even been considered, were surprising to us.

Most of these studies were carried out by using German or Finnish vowels. Developmental research on language acquisition suggests that humans have established prototypes of phonemes in their languages in early childhood and reduced sensitivity to nonnative phonemes [10,11]. Therefore, vowel-sensitive neural substrates, which have been optimized during language learning, may vary across different languages. It is thus essential for a line of research on vowel sound processing to accumulate further information about interindividual variability and intraindividual stability in other languages, such as Japanese, which is characterized by a smaller number of vowels compared with previously studied languages. Research on Japanese phoneme processing has, however, been limited [4]. In the present study, we investigated the cortical representation of Japanese vowels.

The purpose of this study was to demonstrate the cortical representation of Japanese vowels and to examine its similarity with the previous findings in other languages. The stimuli used in this line of research varied across studies. Some employed synthesized vowels [1–4,6,8] or semisynthesized vowels [5] to control the acoustic parameters and to facilitate the examination of formant interaction. In others, naturally spoken vowels were used to investigate the role of phonological features [6] or spectral envelopes [9]. Some psychophysical experiments suggest that spectral cues other than formant frequencies may also be crucial for vowel perception [12]. Thus, we employed digitally recorded vowels spoken by a professional announcer as stimuli. These vowels were well controlled in loudness and pitch, maintaining whole spectral information, which might keep their cortical representation dispersive, and they are purposefully suitable for the present study.

We investigated N1m peak latency and ECD locations for the vowel sounds in a single participant first, because we had to elucidate intraindividual replication to check the reliability of the experimental procedures. We then examined the interindividual consistency in processing Japanese vowels.

Methods

Eight native Japanese speakers (24–57 years old, mean 37, four men and four women) who had normal hearing participated in the experiment. Seven were assessed right-handed with the Edinburgh inventory; laterality quotient ranged from 57.9 to 100, except for one ambidextrous

participant whose laterality quotient was 0. One of the right-handed participants (a 28-year-old woman) participated in experiments for intraindividual replication. All participants were fully informed of the methods and techniques of noninvasive MEG recordings before signing a written agreement to participate. The procedure used in the study was approved by the Ethics Committee of the University of Tokyo.

The stimuli were five Japanese vowels ([a], [e], [i], [o], and [u]) separately uttered by a female speaker. The frequencies of the first (F1) and second (F2) formants of these vowels were as follows: [a]: 1140, 1590 Hz; [e]: 590, 2590 Hz; [i]: 390, 3080 Hz; [o]: 600, 1000 Hz; and [u]: 380, 2100 Hz. The waveform of each vowel was trimmed and naturally tapered to have the same duration of 290 ms from voice onset. The five vowels were presented with equal probability in a pseudorandom order, with the stipulation that the same vowel could not appear consecutively. The stimuli were sequenced by the STIM2 system (Compumedics Neuroscan, El Paso, Texas, USA) and delivered binaurally at 70 dB sound pressure level above respective hearing thresholds through ER-3A earphones (Etymotic Research, Elk Grove Village, Illinois, USA) at a stimulus onset asynchrony of 1.5 s. During the experiment, the participants were instructed to look at the gaze point and to press a plastic button with their right forefinger whenever [e] appeared.

Auditory-evoked magnetic fields were recorded in a sound-attenuated magnetically shielded room by the use of VectorView (Elekta Neuromag, Helsinki, Finland), which has 204 planar first-order gradiometers at 102 measurement sites on a helmet-shaped surface that covers the entire scalp. Auditory stimulus-triggered epochs of 1050 ms duration (including a 50-ms prestimulus baseline) were filtered online with a bandpass of 1.0–200.0 Hz and recorded at a sampling rate of 600.0 Hz. Epochs with artifacts exceeding 3 pT/cm in any channel were excluded from averaging. Erroneous epochs were discarded when the participants failed to push the button at [e] or mistakenly pushed it at the other four vowels. In one session, at least 250 artifact-free epochs were recorded per vowel and were selectively averaged for analysis. Eight sessions were repeatedly measured for the single participant, extending over several days. For the rest of the participants, a single session was carried out.

Data analyses were performed on the responses to the vowels [a], [i], [o], and [u]. The averaged waveforms were filtered off-line with a low pass at 40 Hz, and the mean amplitude from −50 to 0 ms in a prestimulus period was defined as the baseline for each channel. The peak latency of the N1m component was determined for each hemisphere by the time point at which the root-mean-square of the selected perisylvian channels (Fig. 1a) reached maximum, from 80 to 140 ms, after the stimulus onset. The sources of each N1m component were modeled separately as a single ECD for each hemisphere. The ECDs were calculated independently for vowels and sessions in each participant at the peak latencies from the same perisylvian channels. The ECDs with goodness of fit above 75% were adopted.

Before data acquisition, magnetic resonance imaging (MRI) scans were obtained from all participants. Referenced points (nasion and bilateral preauricular points) and the scalp of each participant were digitized by an Isotrak II system (Polhemus, Colchester, Vermont, USA) to coregister the MEG coordinate system onto the individual MRI. The MEG results were imported into BESA 5.1.2 (MEGIS Software, Gräfelfing, Germany) and transformed into Talairach space by using the interactive link with BESA 5.1.2 and BrainVoyager QX (Brain Innovation B.V., Maastricht, The Netherlands). The MEG results were presented in Talairach coordinates to normalize interindividual anatomical variability in the present study.

Intraindividual analyses of the data for the single participant across eight sessions and interindividual analyses of the data across eight participants were performed. ECD parameters for the N1m responses to each vowel were statistically analyzed in each hemisphere by a repeated-measures analysis of variance and post-hoc Scheffé comparisons. We considered $P<0.05$ to be statistically significant for these analyses. A Greenhouse–Geisser correction was performed when appropriate.

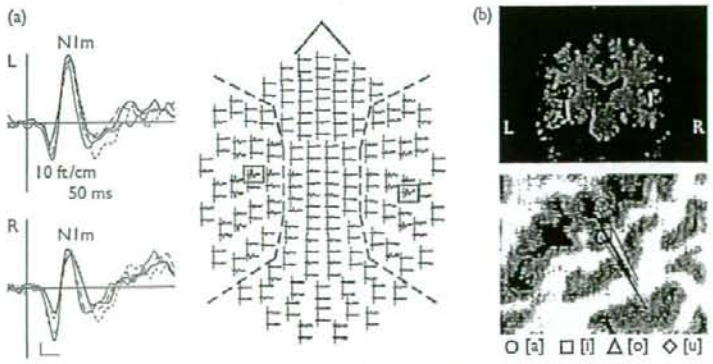

Fig. 1 The averaged N1m response waveforms elicited by the vowels [a] (thin lines), [i] (thick lines), [o] (dashed lines), and [u] (dotted lines) in a representative participant. The perisylvian channels in each hemisphere are bordered with dashed lines (a). The equivalent current dipole locations for N1m from the single participant in one particular session are presented in the axial plane and in the left parasagittal plane of the magnetic resonance image. Each symbol represents the dipole for different vowels. The black tails represent dipole orientation (b).

Table 1 Mean (and SEM) (n=8) of the N1m ECD parameters in intraindividual study

	Left hemisphere					Right hemisphere				
	Latency (ms)	x (mm)	y (mm)	z (mm)	Orientation (deg)	Latency (ms)	x (mm)	y (mm)	z (mm)	Orientation (deg)
[a]	106.4 (0.9)	−43.2 (0.7)	−31.5 (0.8)	10.0 (1.6)	112.7 (1.4)	111.4 (0.9)	54.8 (0.5)	−30.5 (1.1)	12.1 (0.6)	128.9 (2.0)
[i]	111.4 (0.9)	−43.3 (1.2)	−30.5 (0.8)	5.0 (1.1)	117.3 (1.4)	115.1 (1.3)	49.6 (1.0)	−29.3 (1.1)	8.5 (1.6)	128.6 (1.8)
[o]	113.2 (0.9)	−43.9 (0.8)	−30.1 (0.8)	9.7 (1.6)	113.5 (1.1)	118.8 (1.5)	53.9 (1.2)	−29.7 (1.1)	12.9 (1.2)	133.9 (2.4)
[u]	116.3 (0.9)	−42.5 (0.8)	−31.0 (0.7)	2.4 (1.0)	117.2 (1.2)	118.2 (0.9)	50.5 (1.1)	−33.0 (0.7)	5.0 (1.3)	124.4 (1.8)
F-value	31.04	1.07	2.95	26.00	8.01	13.40	10.35	5.76	14.75	6.04
P-value	0.000002	0.37	0.082	0.000025	0.0032	0.0015	0.0025	0.023	0.000067	0.020

Orientation [$=180+\tan^{-1}(Qz/Qy)$]: a downward rotation of the yz-plane projection of the ECD moment (Q) from the y-axis.
ECD, equivalent current dipole.

Table 2 Mean (and SEM) (n=8) of the N1m ECD parameters in interindividual study

	Left hemisphere					Right hemisphere				
	Latency (ms)	x (mm)	y (mm)	z (mm)	Orientation (deg)	Latency (ms)	x (mm)	y (mm)	z (mm)	Orientation (deg)
[a]	103.8 (3.0)	−53.3 (1.2)	−21.5 (5.6)	18.1 (5.9)	111.2 (1.8)	102.6 (3.0)	56.3 (1.0)	−19.4 (5.9)	15.3 (6.1)	121.5 (3.5)
[i]	102.6 (4.5)	−53.3 (1.4)	−20.7 (5.9)	15.6 (5.7)	118.1 (2.3)	102.0 (3.5)	53.8 (1.6)	−18.1 (5.3)	16.3 (5.7)	119.3 (5.1)
[o]	108.9 (3.9)	−53.4 (1.8)	−20.8 (5.5)	17.6 (5.7)	113.7 (2.2)	107.6 (3.7)	54.3 (1.7)	−17.1 (5.1)	16.1 (5.9)	123.2 (5.6)
[u]	111.4 (3.9)	−51.8 (1.2)	−21.2 (5.5)	15.0 (5.4)	114.6 (3.4)	108.2 (2.5)	54.6 (1.6)	−18.5 (5.4)	14.1 (5.9)	119.9 (4.7)
F-value	6.70	1.69	0.54	3.80	4.96	3.79	1.25	1.69	1.49	0.48
P-value	0.0097	0.22	0.63	0.061	0.017	0.066	0.32	0.22	0.26	0.65

ECD, equivalent current dipole.

Results

The behavioral data of a button press revealed that every participant achieved the correct rate of more than 97% (average±SEM: 98.0±0.4), and every participant showed prominent deflections of the N1m responses to each vowel. The responses were well confined in bilateral perisylvian areas (Fig. 1a). The ECDs for N1m were calculated with goodness of fit above 78% (92.2±0.6) and were localized in the superior temporal plane of the MRI of each participant (Fig. 1b).

The averaged ECD parameters obtained from repeated measurements of the single participant are summarized in Table 1. The very small P-values in many parameters mean that the experimental procedures of our study were highly reliable.

The averaged ECD parameters in interindividual analyses are summarized in Table 2. The analysis of variance of the N1m latency revealed a significant difference across vowel types only in the left hemisphere; post-hoc Scheffé comparisons revealed that the vowels [a] and [i] elicited earlier N1m responses than [u]. The ECD orientation across vowel types showed a significant difference only in the left hemisphere; the orientation for [i] was more posteriorly oriented than [a] by approximately seven degrees in the parasagittal plane. In the inferosuperior (z) axis, although it did not reach a significant level, the N1m location for [a] showed a tendency to be superior to those for other vowels. Other ECD parameters were not significantly different across vowel types in either hemisphere. We also examined Euclidean distances between every pair of the vowel ECD locations with and without normalization by the mean distance. No significant difference in distances was, however, observed between any vowel pairs. Furthermore, we compared a displacement of each vowel from the mean ECD location for all vowels with and without normalization by the mean displacement. No significant difference in displacements was, however, detected across vowels. This statistical insignificance was replicated even when the ambidextrous participant was excluded from the analyses.

Discussion

In intraindividual analyses for the single participant, the ECD locations and orientations did show a significant difference in both hemispheres with very small P-values. Well-replicated results confirmed the reliability of the experimental procedures in the present study, and they also supported the existence of cortical maps during the processing of vowels that were pointed out by Eulitz *et al.* [3] in the preceding study.

The interindividual analysis revealed that the N1m latency for [u] was significantly longer than that for [a] in the left hemisphere. The intraindividual analysis showed similar results; the N1m latency for [a] was significantly shorter than those for [i], [o], and [u] in the left hemisphere. Previous studies adopted the N1m component as an index of processing activity in the auditory cortex. N1m latency reflects temporal encoding, which is a critical element of neuronal activity. Roberts *et al.* [13] and Roberts and Poeppel [14] reported that N1m latency for lower-frequency sinusoidal tones was prolonged compared with higher-frequency tones. The results of the studies using vowel stimuli suggested that N1m latency for vowels depends on

the position of F1 and can be interpreted in terms of the sinusoidal data [1,8]. Vowel [a] with relatively high F1 elicited an earlier N1m response than [i] or [u], both of which had a relatively low F1. The results of the present study were in line with this notion.

In the present study, the ECD orientation showed the significant main effect of vowels. In the parasagittal plane, the ECD for [i] was more posteriorly oriented than [a] by approximately 7° in the left hemisphere. Preceding studies on the tonotopic organization with pure tones [15–17] and with syllables [7] also found an ECD orientation shift. As the ECD orientation depends on the underlying cortical structure (i.e. the direction of apical dendrites of activated neurons), it contains physiologically important information, which is unique to electromagnetic measurement. The target areas that were focused on in this line of study were characterized by their folded shapes. The ECD rotation suggested that the centroids of vowel processing were close to one another and that they slightly shifted along Heschl's gyrus in the left hemisphere.

It must be noted that in interindividual analyses, the significant main effects in N1m latency and ECD orientation were shown only in the left hemisphere. This may imply left hemispheric predominance in vowel processing [1,5]. It is widely known in the first place that an interhemispheric asymmetry exists in the superior temporal gyrus. The left hemisphere is mainly involved in temporal processing, although the right hemisphere's forte is processing spectral information [18,19]. The greater volumes of white matter in the left hemisphere, which can be attributed to the difference in myelination, explain the rapid processing of auditory stimuli and a left hemisphere dominance for speech [20–22]. The results of the present study suggest that not only spectral but also temporal information processing plays an important role in vowel perception.

In interindividual analyses for the eight participants, a difference in ECD locations across vowels did not reach a significant level. For one thing, the relatively small number of participants might be the cause. We should acknowledge that the number is smaller in our study than those in preceding studies. Furthermore, the characteristics of Japanese might contribute to the results. Some researchers suggested that, in infancy, exposure to particular phonemes leads to neural sensitivity to these phonemes, and consequently the non-native phonemes cannot be discriminated in adults [23–25]. These results may lead to the notion that vowel processing is affected by exposure to a language-specific phonological format in early life. The number of vowels in Japanese is five and is fewer than those in the other languages studied in previous research. If the neural substrates for vowel processing in the auditory cortex are inherently limited, a language with fewer vowels may be allowed to use the same amount of neural substrates with more degrees of freedom. This notion is also applicable to the motor control of articulation. A language with fewer vowels widely allocated in the same F1–F2 space is allowed a relatively coarse control of articulation. The sparse allocation of sensorimotor neural representation of Japanese vowels may consequently result in some interindividual variability and lead to difficulties in identifying consistent ECD locations for each vowel across the participants. This notion does not, however, contradict the existence of an individual cortical map for vowels in Japanese, considering that stable patterns of vowel ECD sources were observed in the single participant.

Conclusion

In the current study, intraindividual replication of the ECD locations and orientations supported the existence of phoneme-specific cortical maps for Japanese. ECD parameters did not, however, reach a significant level except for the ECD orientation in the left hemisphere in the interindividual analyses. Further information on the vowel processing of various languages is awaited because vowel density in the spectral space may be reflected in the cortical map.

Acknowledgments

The authors wish to thank Keiko Yamakawa and Tomomi Mizuochi for their helpful comments. We especially thank Yusuke Akamatsu for providing the stimulus materials.

References

1. Diesch E, Eulitz C, Hampson S, Ross B. The neurotopography of vowels as mirrored by evoked magnetic field measurements. *Brain Lang* 1996; 53:143–168.
2. Eulitz C, Diesch E, Pantev C, Hampson S, Elbert T. Magnetic and electric brain activity evoked by the processing of tone and vowel stimuli. *J Neurosci* 1995; 15:2748–2755.
3. Eulitz C, Obleser J, Lahiri A. Intra-subject replication of brain magnetic activity during the processing of speech sounds. *Brain Res Cogn Brain Res* 2004; 19:82–91.
4. Kuriki S, Murase M. Neuromagnetic study of the auditory responses in right and left hemispheres of the human brain evoked by pure tones and speech sounds. *Exp Brain Res* 1989; 77:127–134.
5. Mäkelä AM, Alku P, Tiitinen H. The auditory N1m reveals the left-hemispheric representation of vowel identity in humans. *Neurosci Lett* 2003; 353:111–114.
6. Obleser J, Elbert T, Lahiri A, Eulitz C. Cortical representation of vowels reflects acoustic dissimilarity determined by formant frequencies. *Brain Res Cogn Brain Res* 2003; 15:207–213.
7. Obleser J, Lahiri A, Eulitz C. Auditory-evoked magnetic field codes place of articulation in timing and topography around 100 milliseconds post syllable onset. *Neuroimage* 2003; 20:1839–1847.
8. Poeppel D, Phillips C, Yellin E, Rowley HA, Roberts TP, Marantz A. Processing of vowels in supratemporal auditory cortex. *Neurosci Lett* 1997; 221:145–148.
9. Shestakova A, Brattico E, Soloviev A, Klucharev V, Huotilainen M. Orderly cortical representation of vowel categories presented by multiple exemplars. *Brain Res Cogn Brain Res* 2004; 21:342–350.
10. Cheour M, Ceponiene R, Lehtokoski A, Luuk A, Allik J, Alho K, *et al.* Development of language-specific phoneme representations in the infant brain. *Nat Neurosci* 1998; 1:351–353.
11. Kuhl PK, Williams KA, Lacerda F, Stevens KN, Lindblom B. Linguistic experience alters phonetic perception in infants by 6 months of age. *Science* 1992; 255:606–608.
12. Ito M, Tsuchida J, Yano M. On the effectiveness of whole spectral shape for vowel perception. *J Acoust Soc Am* 2001; 110:1141–1149.
13. Roberts TP, Ferrari P, Stufflebeam SM, Poeppel D. Latency of the auditory evoked neuromagnetic field components: stimulus dependence and insights toward perception. *J Clin Neurophysiol* 2000; 17:114–129.
14. Roberts TP, Poeppel D. Latency of auditory evoked M100 as a function of tone frequency. *NeuroReport* 1996; 7:1138–1140.
15. Cansino S, Ducorps A, Ragot R. Tonotopic cortical representation of periodic complex sounds. *Hum Brain Mapp* 2003; 20:71–81.
16. Pantev C, Bertrand O, Eulitz C, Verkindt C, Hampson S, Schuierer G, *et al.* Specific tonotopic organizations of different areas of the human auditory cortex revealed by simultaneous magnetic and electric recordings. *Electroencephalogr Clin Neurophysiol* 1995; 94:26–40.
17. Tiitinen H, Alho K, Huotilainen M, Ilmoniemi RJ, Simola J, Näätänen R. Tonotopic auditory cortex and the magnetoencephalographic (MEG)

equivalent of the mismatch negativity. *Psychophysiology* 1993; 30: 537–540.
18. Belin P, Zilbovicius M, Crozier S, Thivard L, Fontaine A, Masure MC, *et al.* Lateralization of speech and auditory temporal processing. *J Cogn Neurosci* 1998; 10:536–540.
19. Zatorre RJ, Belin P. Spectral and temporal processing in human auditory cortex. *Cereb Cortex* 2001; 11:946–953.
20. Anderson B, Southern BD, Powers RE. Anatomic asymmetries of the posterior superior temporal lobes: a postmortem study. *Neuropsychiatry Neuropsychol Behav Neurol* 1999; 12:247–254.
21. Galuske RA, Schlote W, Bratzke H, Singer W. Interhemispheric asymmetries of the modular structure in human temporal cortex. *Science* 2000; 289:1946–1949.
22. Penhune VB, Zatorre RJ, MacDonald JD, Evans AC. Interhemispheric anatomical differences in human primary auditory cortex: probabilistic mapping and volume measurement from magnetic resonance scans. *Cereb Cortex* 1996; 6:661–672.
23. Dehaene-Lambertz G. Electrophysiological correlates of categorical phoneme perception in adults. *NeuroReport* 1997; 8:919–924.
24. Dehaene-Lambertz G, Dupoux E, Gout A. Electrophysiological correlates of phonological processing: a cross-linguistic study. *J Cogn Neurosci* 2000; 12:635–647.
25. Näätänen R, Lehtokoski A, Lennes M, Cheour M, Huotilainen M, Iivonen A, *et al.* Language-specific phoneme representations revealed by electric and magnetic brain responses. *Nature* 1997; 385: 432–434.

International Journal of Pediatric Otorhinolaryngology (2007) 71, 1105–1115

ELSEVIER

International Journal of Pediatric Otorhinolaryngology

www.elsevier.com/locate/ijporl

Early myelination patterns in the brainstem auditory nuclei and pathway: MRI evaluation study

Masaki Sano [a,*], Kimitaka Kaga [a], Chen-Chieh Kuan [a], Kenji Ino [b], Kazuo Mima [b]

[a] *Department of Otorhinolaryngology and Head & Neck Surgery, Graduate School of Medicine and Faculty of Medicine, University of Tokyo, 7-3-1 Hongo, Bunkyo-ku, Tokyo 113-8655, Japan*
[b] *Division of Radiology, University of Tokyo Hospital, Tokyo, Japan*

Received 1 December 2006; received in revised form 1 April 2007; accepted 2 April 2007

KEYWORDS
Myelination;
MRI study;
Brainstem;
Auditory nuclei and pathway

Summary

Objective: The purpose of this study is to investigate the early myelination patterns of brainstem auditory nuclei and pathway on magnetic resonance imaging compared with past histological research. We aimed to identify the time course difference in myelination of the brainstem auditory nuclei and pathway between magnetic resonance imaging and histological research results.
Methods: Subjects were 192 infants ranging in age from −4 to 224 corrected postnatal weeks. Images were obtained using a 1.5 T magnetic resonance unit. In four sites (cochlear nucleus, superior olivary nucleus, lateral lemniscus, inferior colliculus) of the brainstem auditory nuclei and pathway on four cross-sections obtained perpendicular to the long axis of the brainstem, signal changes of T1- and T2-weighted magnetic resonance images were analyzed using a region-of-interest methodology according to corrected postnatal age.
Results: The cochlear nucleus and superior olivary nucleus showed myelinated intensity change from −3 to 13 corrected postnatal weeks on T2-weighted images. The lateral lemniscus showed myelinated intensity change from −3 to 8 corrected postnatal weeks on T1-weighted images and from −1 to 13 corrected postnatal weeks on T2-weighted images. The inferior colliculus showed myelinated intensity change from −2 to 39 corrected postnatal weeks on T2-weighted images.
Conclusions: Magnetic resonance imaging revealed the signal intensity change by myelination 11–18 weeks later than those reported in the histological literature. This time lag suggests that apart from histological research, the necessity for the milestones of auditory pathway maturation using MRI is suggested to evaluate the development of brainstem auditory pathway using MRI. This result suggests that myelination does not take place suddenly but happens gradually, so definite

* Corresponding author. Tel.: +81 3 5800 8665; fax: +81 3 3814 9486.
E-mail address: neurootolsano@ybb.ne.jp (M. Sano).

0165-5876/$ – see front matter
doi:10.1016/j.ijporl.2007.04.002

myelination, namely the complete change of myelin sheath ingredients, loss of water, and gain of lipids, is needed to be detected by magnetic resonance imaging.

1. Introduction

The degree of myelination in the brainstem auditory nuclei and pathway has been studied histologically and physiologically as a parameter of auditory system maturation in early childhood [1–7]. Yakovlev and Lecours [2] found that the statoacoustic system begins myelination at the end of the fifth fetal month. Rorke and Riggs [3] found that in mature newborns, the superior olivary nucleus and the lateral lemniscus are myelinated, while the inferior colliculus is only slightly myelinated. Moore et al. [4] reported on the brainstem histology that the cochlear nucleus, superior olivary nucleus, lateral lemniscus, and inferior colliculus undergo myelination between the 26th and 29th fetal weeks; from the 29th fetal week, the density of myelination (thickness of myelin sheaths) increases in all pathways until at least 1 year postnatal age.

The increasing speed of fiber conduction involving the auditory brainstem nuclei and pathway can be measured by auditory brainstem response (ABR). Many researchers [5–9] have described a decrease in peak and interpeak latencies of ABR in early infancy and attributed the phenomenon to myelination of the brainstem auditory nuclei and pathway.

However, previous reports have not mentioned magnetic resonance imaging (MRI) to assess the brainstem auditory nuclei and pathway. Observation of myelination *in vivo* using computed tomography (CT) has been attempted [10–12], but neither density resolution nor space resolution was sufficient for evaluation of myelination. Such techniques have been replaced by MRI, which offers considerably more information about myelination [13–23]. Magnetic resonance imaging is useful to evaluate the central nervous system myelination as shown by signal intensity changes. The most important anatomical structures of the brainstem auditory nuclei and pathway are the cochlear nucleus, superior olivary nucleus, lateral lemniscus, and inferior colliculus. With the progress of myelination, the signal intensity of MRI changes from low to high on T1-weighted imaging and from high to low on T2-weighted imaging [24–28].

The purpose of this study is to investigate the early myelination patterns of the brainstem auditory nuclei and pathway on MRI compared with the previous histological research.

2. Patients and methods

2.1. Patients

Among infants who underwent brain MRI between 2000 and 2005 at the University of Tokyo Hospital, subjects were 192 neonates, infants, and small children (98 boys, 94 girls) with a mean age of 8.7 weeks (range, −4 to 224 weeks by corrected postnatal weeks; negative weeks means a premature infant; Fig. 1). These patients underwent MRI because a brain disorder was suspected. Images demonstrating anomalies, infarcts, or hemorrhages in the brainstem were excluded from the study. No brainstem lesions or severe central nervous system malformation were apparent in any subject of this study.

2.2. Imaging methods

This study used 1.5 T MR units (Magnetom Vision 1.5T, Siemens, Germany; Signa Excite HD 1.5T, GE, USA). T1-weighted images were obtained using spin-echo or inversion recovery sequences and T2-weighted images were obtained using spin-echo sequences. Sections were perpendicular to the long axis of the brain and were 5–7 mm thick. Repetition time (TR) is 300–600 ms in T1-weighted images and 3000 ms in T2-weighted images. Echo time (TE) was 10–20 ms in T1-weighted images and 70–100 ms in T2-weighted images.

2.3. Evaluation methods

Magnetic resonance imaging is useful to evaluate myelination in the central nervous system [13]. Magnetic resonance imaging also allows the fine internal structure of the brainstem to be seen directly [27]. The changes in signal intensity that are associated with myelination on T1- and T2-weighted images are due to changes in the lipid and water contents of developing myelin [15,28]. On T1-weighted imaging, signal intensity progresses from hypo- to hyperintensity when myelination occurred and becomes distinguishable as a hyperintense area. On T2-weighted imaging, signal intensity progresses from hyper- to hypointensity when myelination occurred and becomes distinguishable as a hypointense area [18,23,24]. However, developing surrounding tissue may begin to display similar

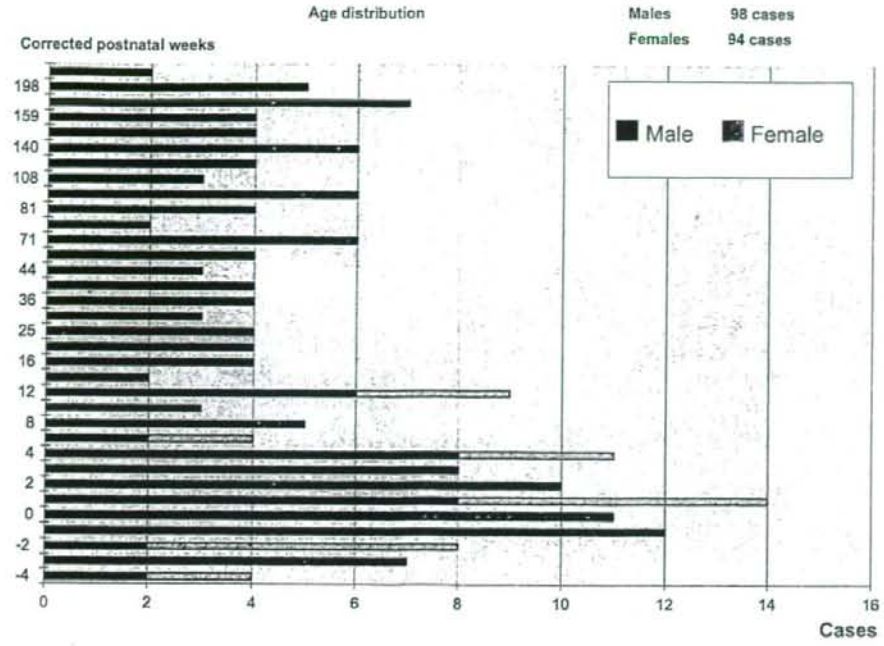

Fig. 1 Histogram shows the age distribution of MRI subjects.

signal intensity to those of the nucleus or tract and the nucleus or tract becomes difficult to distinguish from surrounding tissue on MRI, a phenomenon known as blurring [13]. Blurring is a phenomenon in which the myelination of gray matter nuclei (cochlear nucleus, superior olivary nucleus, and inferior colliculus) and white matter tracts (lateral lemniscus) proceeds to the surrounding white or gray matter, but later the structures become indistinguishable because of the progress of myelination in the surrounding white or gray matter.

The present study examined 1536 magnetic resonance images (192 cases with eight slices each by T1- and T2-weighted imaging) and analyzed the progress patterns of myelination at four different checking points (cochlear nucleus, superior olivary nucleus, lateral lemniscus, and inferior colliculus) according to region-of-interest (ROI)-based analysis.

2.4. Depiction of regions of interest

Regions of interest were identified in the brainstem auditory nuclei and pathway nucleus and tract with each surrounding area. The identification of the structure was confirmed by consulting a fetal neuroanatomy textbook [29] and a previous study on term neonates [22]. Fig. 2-1 indicates the cochlear nucleus (circle) and surrounding white matter (double circle) in a slice of the brainstem at the pontomedullary junction. Fig. 2-2 indicates the superior olivary nucleus (circle) and surrounding white matter (double circle) in a slice of the brainstem at the pontomedullary junction. Fig. 2-3 indicates the lateral lemniscus (circle) and surrounding gray matter (double circle) in a slice of the brainstem at the isthmus of the 4th ventricle.

Fig. 2-4 indicates the inferior colliculus (circle) and surrounding white matter (double circle) in a slice of the brainstem at the junction of the pons and mesencephalon.

2.5. ROI-based analysis

Counts for each ROI were measured using Centricity Web-J software (GE Yokogawa Medical System Co. L., Tachikawa, Japan). The signal intensity ratio (SIR) was defined as a difference in ROI values between each assessment site of the brainstem auditory nuclei and pathway and the corresponding surrounding tissue.

Signal intensity ratio was calculated as ((ROI value of assessment site − ROI value of surrounding tissue)/ROI value of the assessment site) × 100.

For example, if the ROI value of the inferior colliculus was 1000 and the ROI value of surrounding tissue was 800, SIR = ((1000 − 800)/1000) × 100 = 20.

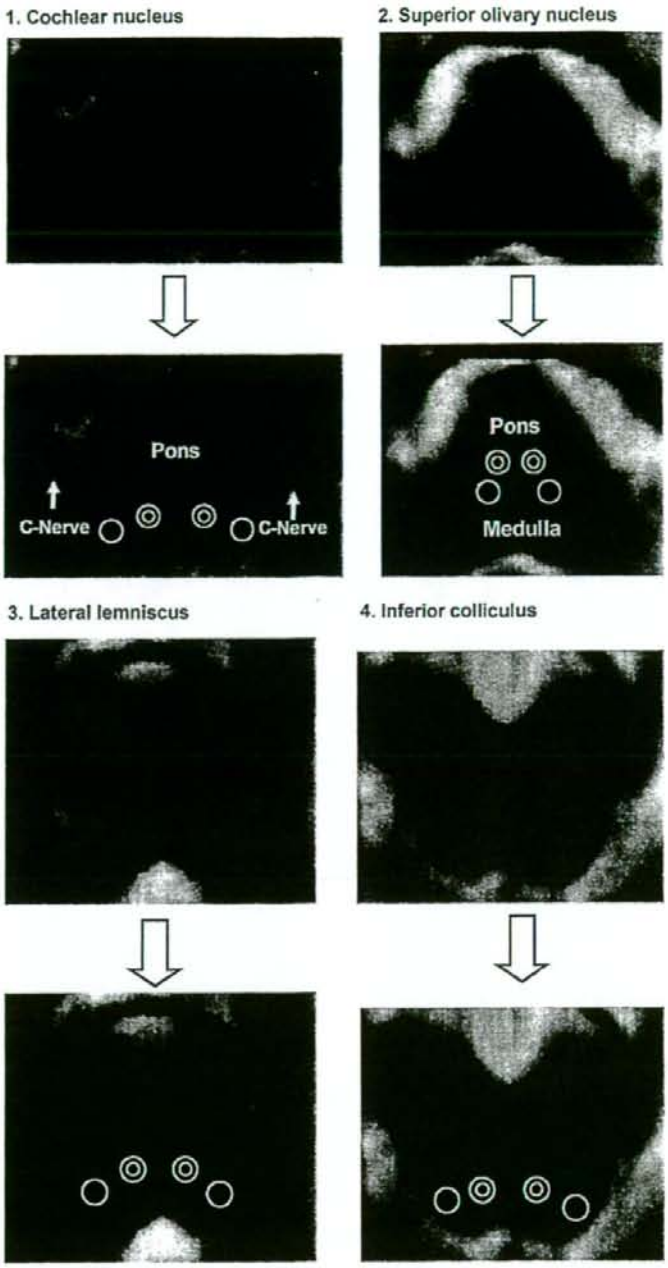

Fig. 2 Depiction of regions of interest (T2-weighted images). A circle is placed at each point of the brainstem auditory nuclei and pathway (cochlear nucleus, superior olivary nucleus, lateral lemniscus, and inferior colliculus) and a double circle is placed at the surrounding gray or white matter. (1) Cochlear nucleus (circle); an arrow indicates cochlear nerves (C-Nerve). (2) Superior olivary nucleus (circle); the pons and medulla are shown. (3) Lateral lemniscus (circle). (4) Inferior colliculus (circle).

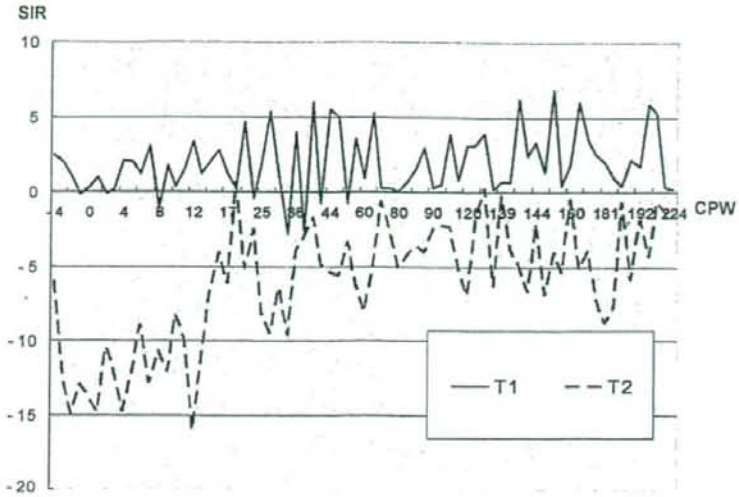

Fig. 3 SIR changes of the cochlear nucleus. Signal intensity ratio (SIR) is: (ROI value of assessment site – ROI value of surrounding tissue/ROI value of the assessment site) ×100. Axis *x*: corrected postnatal weeks (CPW); Axis *y*: signal intensity ratio (SIR).

The SIR value of both sides was measured at each evaluation part and the average value was computed.

2.6. Statistical analysis

We analyzed SIR in relation to corrected postnatal weeks. Corrected postnatal weeks (CPW) are needed for prematurely born infants. The adjustment can be accomplished by subtracting from the current age the number of months that the child was born prematurely. For example, a child born at 28 gestational weeks (3 months before the due date) and imaged at 9 months old should meet the milestones for a 6-month-old (9 – 3) child. Corrected postnatal weeks were calculated according to the definition set by the "Gaining and growing: Calculating corrected age, University of Washington (UW)'s homepage" [30].

The SIR was calculated in each imaging as mentioned in ROI-based analysis using SPSS software, Ver. 14.0 for Windows (SPSS Japan). The mean SIR was calculated at the same corrected postnatal weeks (CPW) and the number of postnatal weeks

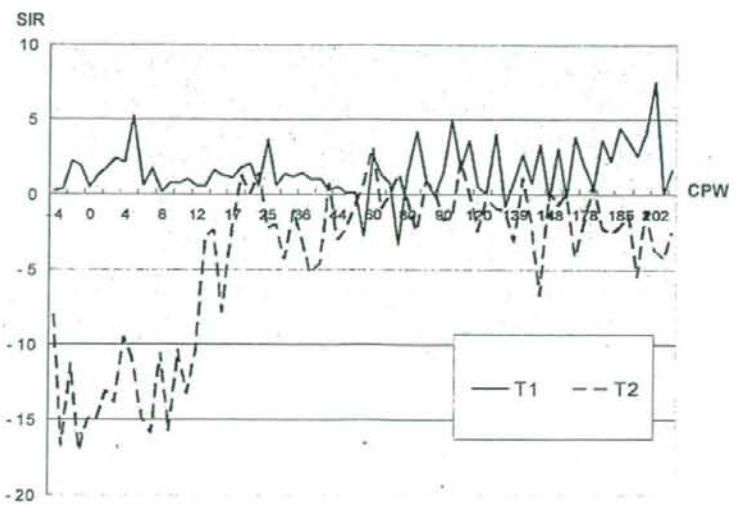

Fig. 4 SIR changes of the superior olivary nucleus.

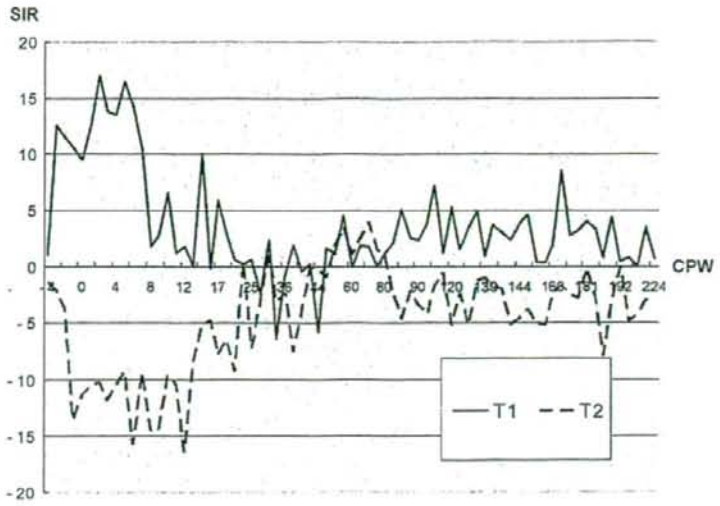

Fig. 5 SIR changes of the lateral lemniscus.

was set on the *x*-axis, with SIR on the *y*-axis using Excel for Windows (Microsoft, Redmond, WA, USA) (Figs. 3–6: a solid line represents T1-weighted imaging, while a dotted line represents T2-weighted imaging). Myelination is shown as a positive and high SIR on T1-weighted imaging and a negative and low SIR on T2-weighted imaging. Blurring is shown as a lower SIR on T1-weighted imaging and a higher SIR on T2-weighted imaging after the myelination period.

In addition, the myelination period was divided by every two or six corrected postnatal weeks and each average SIR value was analyzed using Sigma Stat for Windows software, Version 3.5 (Systat Software, San Jose, CA, USA). One-way factorial ANOVA was used to investigate the difference in average SIR values among each term, followed by Bonferroni's multiple comparison tests for mutual comparison. A *P*-value less than 0.05 denoted the presence of a significant difference.

3. Results

1. The cochlear nucleus did not show any significant differences through all CPW on T1-weighted

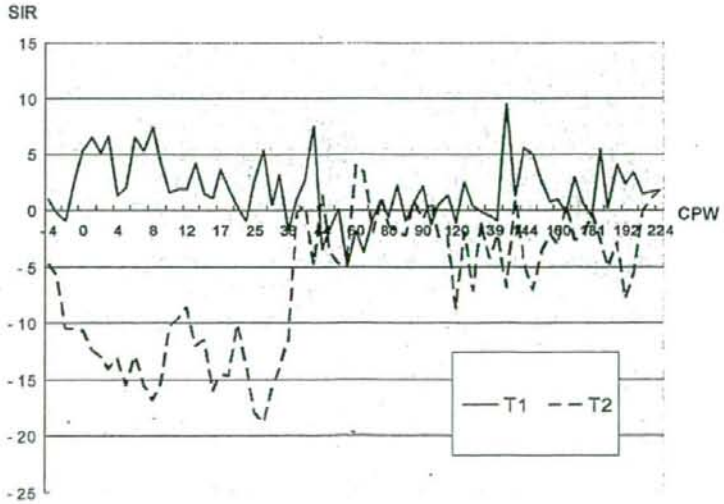

Fig. 6 SIR changes of the colliculus.

imaging ($p > 0.05$), but displayed significant differences between <-3 CPW cases and -3 to 13 CPW cases and between -3 to 13 CPW cases and >13 CPW cases on T2-weighted imaging ($p < 0.05$) (Fig. 3).

2. The superior olivary nucleus also did not show any significant differences through all CPW on T1-weighted imaging ($p > 0.05$), but displayed significant differences between <-3 CPW cases and -3 to13 CPW cases and between -3 to 13 CPW cases and >13 CPW cases on T2-weighted imaging ($p < 0.05$) (Fig. 4).
3. The lateral lemniscus, which is the white matter tract, showed significant differences between <-3 CPW cases and -3 to 8 CPW cases and between -3 to 8 CPW cases and >8 CPW cases on T1-weighted imaging ($p < 0.05$). In T2-weighted imaging, there were significant differences between <-1 CPW cases and -1 to 13 CPW cases and between -1 to 13 CPW cases and >13 CPW cases ($p < 0.05$) (Fig. 5).
4. The inferior colliculus did not show any significant differences through all CPW on T1-weighted imaging ($p > 0.05$), but displayed significant differences between <-2 CPW cases and -2 to39 CPW cases and between -2 to 39 CPW cases and >39 CPW cases on T2-weighted imaging ($p < 0.05$) (Fig. 6).

4. Discussion

4.1. Histological study of myelination

According to Flechsig [1], myelination is one of the prominent morphological parameters for determining functional development in the central nervous system. The brainstem auditory nuclei and pathway are considered to develop myelination in the fetal and early postnatal periods according to various histological studies [2,3,31,32].

Yakovlev and Lecours [2] reported the myelination development of the brain and brainstem. They stained myelin by the Loyez method over 200 cerebra specimens ranging in age scale from the fourth fetal month to one postnatal year. They evaluated the myelination by the appearance of light gray staining and the termination of myelogenesis by the time when the region attained the tinctorial intensity comparable to that in healthy adult brain, and they mentioned that at the end of the fifth fetal month, the superior olivary nucleus, the lateral lemniscus, and the inferior colliculus begin to myelinate and complete myelination at about the middle of the ninth fetal month. Rorke and Riggs [3] reported the myelination of brain tissue in 107 infants; they stained specimens with Luxol fast blue-cresyl violet according to the technique of Kluver-Barrera because this dye has an affinity for lipids of the myelin sheath. They classified specimens as from mature infants or immature infants according to not the fetal weeks but the birth body weight (500–2500 g). Their result is that in immature newborns, the cochlear nucleus is fully myelinated but the superior olivary nucleus, lateral lemniscus, and inferior colliculus are less well myelinated. In mature newborns, the cochlear nucleus, superior olivary nucleus, and lateral lemniscus are fully myelinated, although the inferior colliculus is only slightly myelinated. Moore et al. [4] reported the myelination of the brainstem auditory nuclei and pathway; they stained myelin sheaths using the Nissl cresylecht violet technique and the Woelcke hematoxylin method on 12 fetal and infant brainstems ranging in age from the sixth fetal month to one postnatal year. The age of the fetus was determined by a neuropathologist on the basis of the clinical history and the fissural pattern of the cortex. They mentioned that the cochlear nucleus, superior olivary nucleus, lateral lemniscus, and inferior colliculus undergo myelination between the 26th and 29th fetal weeks; from the 29th fetal week, the density of myelination (thickness of myelin sheaths) increases in all pathways until at least 1 year postnatal age. Staining intensity was also increased in the 33- and 34-week-old fetal brainstems and in the 1 month and 6 month subjects. By 1 year postnatal age, myelin sheaths in the cochlear nerve appear as heavily stained as those in adult material. Regarding the reason for the difference in results between the study by Moore et al. and earlier histological studies, in earlier histological studies based on large numbers of fetal brainstems, fetal age was determined by body size, a parameter that is inherently more variable than maturation. Fetal weeks are thus unlikely to be as accurate as measurements used in their study. In addition, earlier histological studies were performed at a light microscopic level and could not determine an absolute endpoint to the myelination process.

In Table 1 we present the summary of myelination period of brainstem auditory pathway from histological study.

4.2. MRI study of myelination

Presently, MRI is a useful tool to evaluate myelination in the infant brain [13]. Regarding the brainstem auditory nuclei and pathway, how the myelination is reflected on MRI compared with previous histological study results was the purpose of this study. Regarding how myelin is distributed in the

Table 1 Comparison of histological study and MRI study

	CN	SON	LL	IC
Histological study				
Yakovlev and Lecours		23–24th fw (last of 5th fetal month)		
Rorke and Riggs		<40th fw (before mature born)		
Moore		26th and 29th fw		
MRI study				
Martin (2.35 T)	–	–	–	<40th fw (T2)
Counsell (1.0 T)	–	–	26th fw (T1)	25th fw (T2)
Our results (1.5 T)	37th fw (T2)	37th fw (T2)	37th fw (T1)	38th fw (T2)

fw: fetal weeks; CN: cochlear nucleus; SON: superior olivary nucleus; LL: lateral lemniscus; IC: inferior colliculus; T: Tesla.

brainstem auditory nuclei and pathway and why MRI reflects the myelination, past histological research was consulted. Rorke and Riggs [3] presented in their book a photograph of the sharp contrast of myelinating tissue of the cochlear nucleus, superior olivary nucleus, lateral lemniscus, and inferior colliculus with non-myelinating surrounding tissue. Rorke's staining dye has an affinity for lipids of the myelin sheath. T1- and T2-weighted images also reflect the change in the lipid content in the developing myelin sheath. Moore et al. [4] also presented the histology of myelination on the brainstem auditory nuclei and pathway; by 29 fetal weeks, the ventral cochlear nucleus was filled with myelinated axons and the superior olivary nucleus was also visible because of a pervasive fine-fiber myelinated neuropil. Magnetic resonance imaging is considered to detect this myelinated axon congregation and change the signal intensity for a reason that is explained below.

The myelin sheath is composed of multiple layers that are wound radially around the long axis of an axon. Analysis by radiographic diffraction and polarized microscopy has shown that the layers have a characteristic structure: protein–lipid–protein–lipid–protein [33,34]. The changes in signal intensity associated with myelination on T1- and T2-weighted images are due to changes in the lipid and water contents of developing myelin [35]. Myelination is probably shown as high signal intensity on T1-weighted images because of T1 shortening caused by an increase in cholesterol and glycolipids in the myelin sheath. The hypointense appearance of myelination on T2-weighted images corresponds to the time of tightening of myelin around the axon and the saturation of polyunsaturated fatty acids within the myelin membrane [35]. The reduction in signal intensity on T2-weighted images is probably due to a reduction in the number of aqueous protons due to the development of the hydrophobic inner phospholipids layer [35]. Other maturational changes, such as glial cell multiplication, increases in synaptic density, and dendrite formation, occur at the same time as myelination in gray matter nuclei and may reduce the amount of free water at these sites, thereby contributing to the hypointense signal on T2-weighted images [35] (which may be the reason why T2-weighted imaging is more suitable for evaluation of gray matter nuclei). Blurring phenomenon of MRI [13] can be explained from the Moore histological report [4] that compared adult material with fetus material regarding the superior olivary complex; in adult material, myelinated axons fill the surrounding reticular formation and the superior olivary complex becomes less prominent than in the fetal period.

Our MRI study, the cochlear nucleus and the superior olivary nucleus showed myelinational signal change by the time of −3 CPW (37th fetal week) and blurring occurred at least 13 CPW on T2-weighted imaging. The lateral lemniscus, which is the white matter tract, showed myelinational signal change at −3 CPW (37th fetal week) and blurring occurred by at least 8 CPW on T1-weighted imaging. On T2-weighted imaging, myelinational signal change occurred at −1 CPW and blurring occurred by at least 13 CPW. In the inferior colliculus, myelinational signal changes were observed at −2 CPW (38th fetal week) and blurring occurred by at least 39 CPW. Magnetic resonance imaging can detect the myelinational signal intensity change; however, subsequently, blurring occurs and myelination can no longer be detected. In these results, it turned out that it is much later, about 3.5 months (11–18 weeks) than histological research previously demonstrated, that MRI shows signal intensity change. A proposed explanation for this difference is that myelination does not take place suddenly but happens gradually, and after definite myelination with full change of myelin sheath ingredients (loss of water and gain of lipids), it takes a minimal concentration of myelin to have a significant effect on the signal intensity detectable by MRI.

In radiological studies, numerous authors [13,15,19–22,28,36–38] have documented central nervous system changes on MRI corresponding to